

"HIGH ACCURACY RADIATIVE DATA FOR PLASMA OPACITIES"

Sultana N. Nahar
The Ohio State University
Columbus, Ohio, USA



10th International Colloquium on
*"Atomic Spectra and Oscillator Strengths for
Astrophysical and Laboratory Plasmas"*

Berkeley, California, USA

August 3 - 7, 2010

Supports: DOE, NASA, Ohio Supercomputing Center

PLASMA OPACITY

- Opacity determines radiation transport in plasmas
- Opacity is the resultant effect of repeated absorption and emission of the propagating radiation by the constituent plasma elements.
- Radiation energy created in the core (gamma rays) of the sun takes over a million years to travel to the surface: **Reason - OPACITY**
- Microscopically opacity depends on two radiative processes: i) photo-excitation (bound-bound transition) & ii) photoionization (bound-free transition)
- These determine monochromatic opacity $\kappa(\nu)$ at a single photon frequency ν .
- The mean opacity, Rosseland mean opacity, depends also on the physical conditions, such as, temperature, density, elemental abundances and equation of state
- The total $\kappa(\nu)$ is obtained from summed contributions of all possible transitions from all ionization stages of all elements in the source. Calculation of accurate parameters for such a large number of transitions has been the main problem for obtaining accurate opacities.

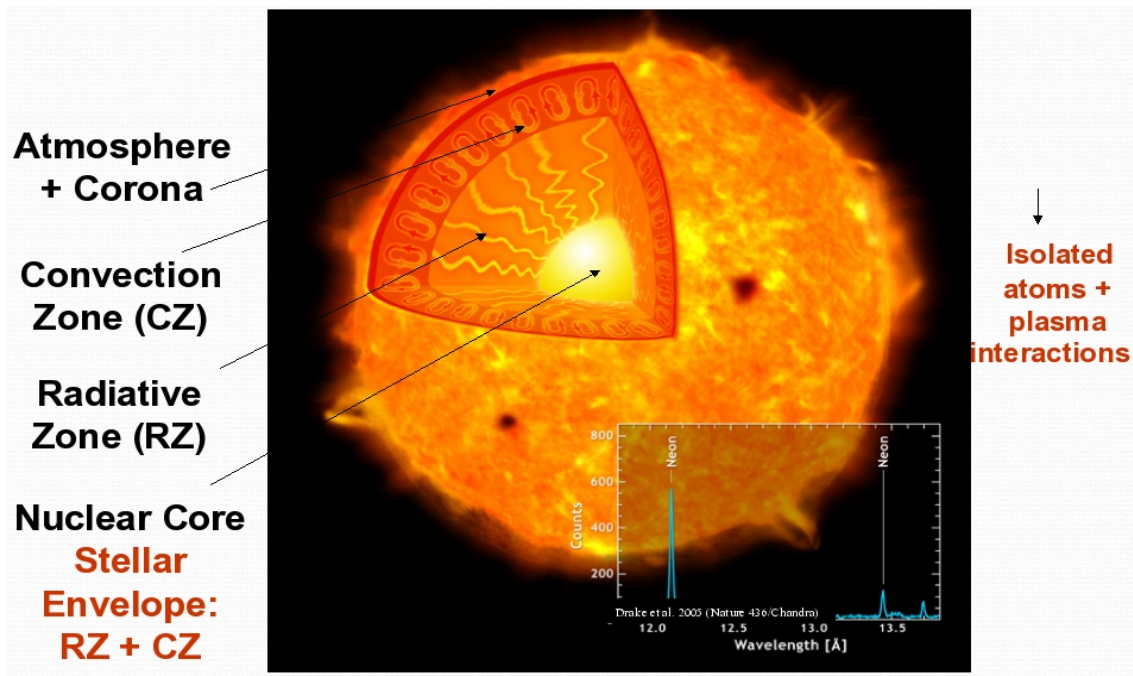
THE OPACITY PROJECT and THE IRON PROJECT: Accurate Study of Atoms & Ions, Applications to Astronomy

- International Collaborations: France, Germany, U.K., U.S., Venezuela, Canada, Belgium
- Earlier opacities were incorrect by factors of 2 to 5 resulting in inaccurate stellar models leading to initiation of the Opacity Project in 1981
- **THE OPACITY PROJECT - OP (1981 - 2006):** study radiative atomic processes (E , f , σ_{PI}) of all elements from H to Fe and calculate opacities in astrophysical plasmas
- **THE IRON PROJECT - IP (1993 -):** collisional & radiative processes of Fe & Fe peak elements
- **RMAX:** Under IP, study X-ray atomic astrophysics
- **Atomic & Opacity Databases (from OP & IP)**
- TOPbase (OP) at CDS:
<http://vizier.u-strasbg.fr/topbase/topbase.html>
- TIPbase (IP) at CDS:
<http://cdsweb.u-strasbg.fr/tipbase/home.html>
- OPserver for opacities at the Ohio Supercomputer Center:
<http://opacities.osc.edu/>
- Latest radiative data at NORAD-Atomic-Data at OSU:
http://www.astronomy.ohio-state.edu/~nahar/nahar_radiativeatomicdata/index.html

OUTCOME OF THE OP & THE IP

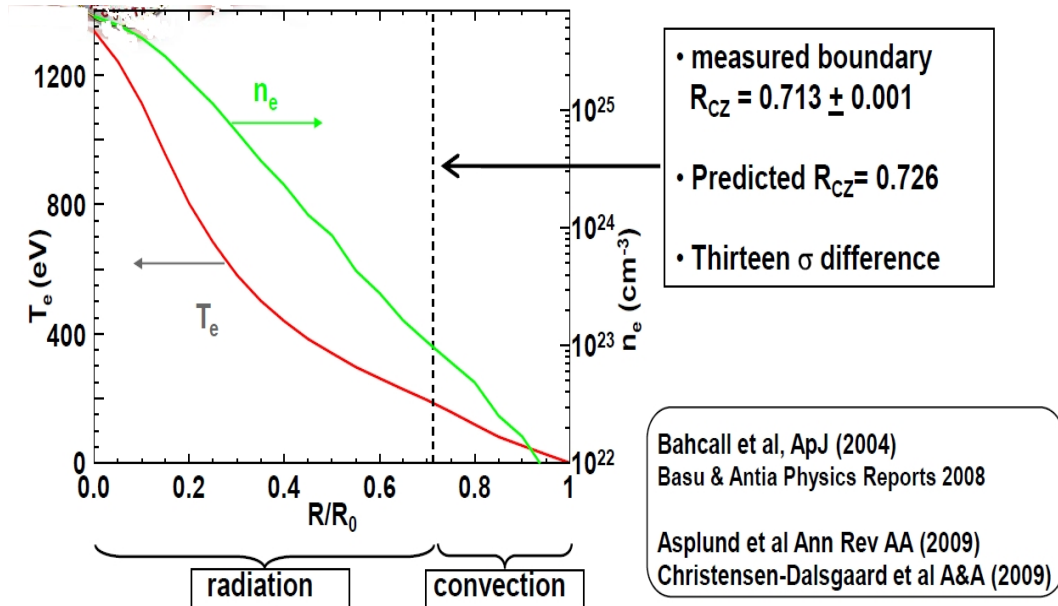
- Results from the OP and IP correspond to the first detailed study for most of the atoms and ions
- New features in photoionization cross sections are revealed
 - OP opacities agreed with those computed under the OPAL, and both solved the outstanding problem on pulsations of cepheids
 - Results from the OP and the IP continue to solve many outstanding problems, e.g., spectral analysis of blackhole environment, abundances of elements, opacities in astrophysical plasmas, dark matter
 - HOWEVER, these are not complete and sufficiently accurate enough to solve all astrophysical problems
 - **Recent developments under the IP:**
 - i) Able to calculate more accurate oscillator strengths for large number of transitions in relativistic Breit-Pauli R-matrix method
 - ii) finding existence of extensive and dominant resonant features in the high energy photoionization cross sections
 - iii) finding important fine structure effects in σ_{PI}

SOLAR OPACITY & ABUNDANCES



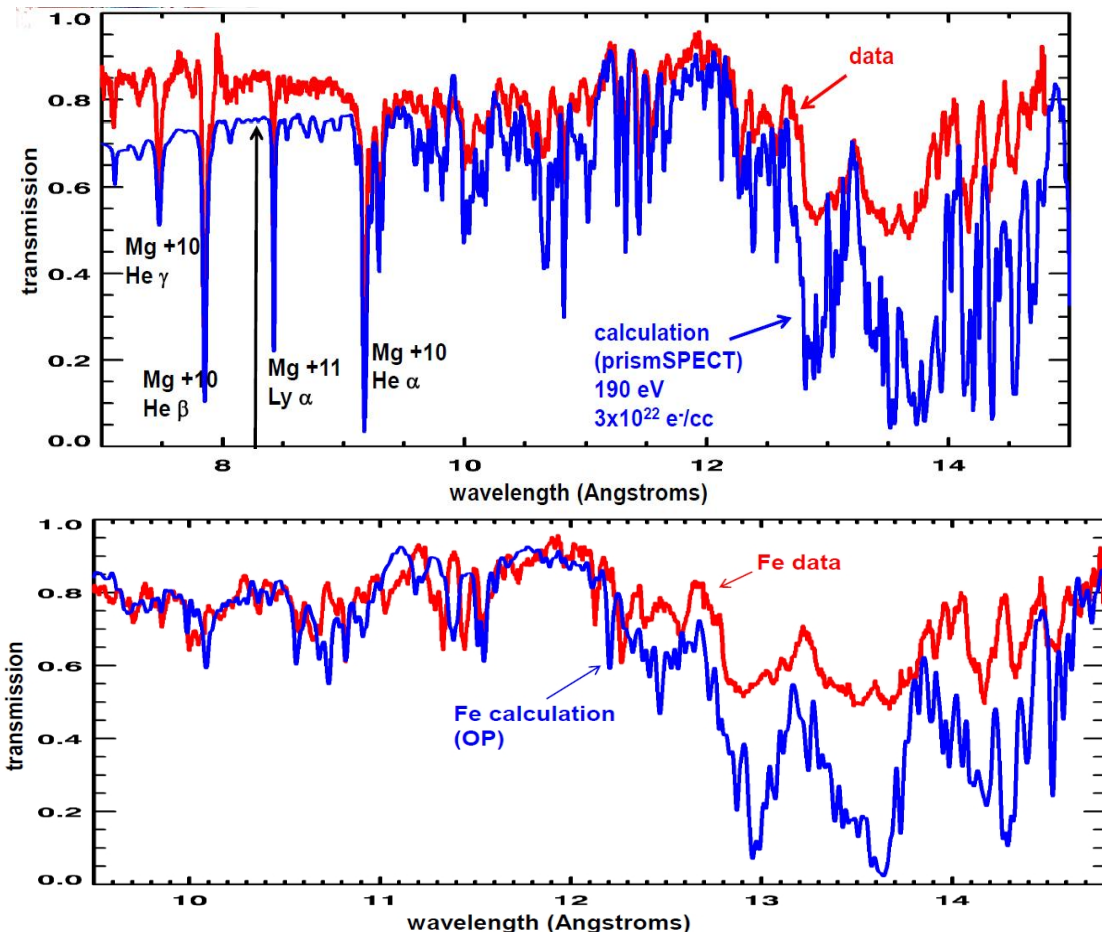
- Although the most studied star, we can not explain all observations.
- Sun's interior - nuclear core to the end of convection zone beyond which the radiation escapes
- At the convection zone boundary, R_{RZ} , the temperature $T_e \sim 193$ eV, density $n_e \sim 10^{23}/cm^3$ (HED condition - NIF, Z-pinch)
- HED condition → important elements: O, Ne, especially Fe (Fe XVII-XIX)
- Radiation transport in the sun depends on the interior opacity (κ) through elemental abundances
- The opacity can determine R_{RZ}

DISCREPANCY IN SOLAR RADIAIVE AND CONVECTION ZONES BOUNDARY (R_{CZ})



- The measured boundary, from helioseismology, of R_{RZ} is 0.713
- The calculated R_{CZ} is 0.726 - large
- A 1% opacity change leads to observable R_{CZ} changes
- Recent determination of abundances of light elements in the sun, C, N and O, are up to 30-40% lower than the standard values, long supported by astrophysical models, helioseismology, and meteoritic measurements
- This is a challenge in accuracy

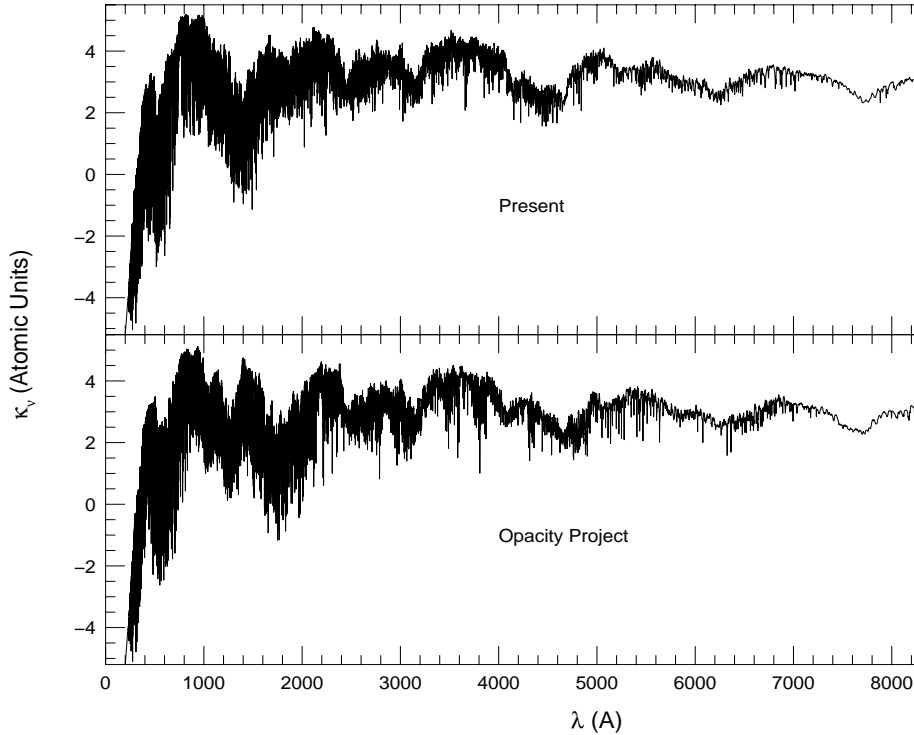
DISCREPANCY BETWEEN EXPERIMENTAL & THEORETICAL OPACITIES (Bailey, Sandia lab)



- Z PINCH spectra at Sandia lab: plasma temperature $T_e \sim 193 \text{ eV}$ & density $n_e \sim 10^{23}/\text{cm}^3$, similar to those at solar R_{CZ}
- Observed (red) and calculated (blue). Top: Diagnostic lines, Bottom: Iron - Large differences **Reason: OPACITY**
- Serious discrepancies for iron opacity using OP data (widely used) & observation
- Experimental n_e is wrong OR bound-free absorption (photoionization) is inaccurate

Monochromatic Opacities κ_ν of Fe IV

(Nahar & Pradhan 2006)



- $\log T = 4.5$, $\log N_e (\text{cm}^{-3}) = 17.0$: condition when Fe IV dominates iron opacity
- κ_ν depends primarily on oscillator strengths (over 710,000 transitions)
- $\kappa_\nu(\text{Fe IV})$ varies over orders of magnitude between 500 - 4000 Å
- Comparison indicates systematic shift in groups of OP energies

DETERMINATION OF OPACITY:

1. Photoexcitation - Photon absorption for a bound-bound transition



- Oscillator Strength (f_{ij})

Monochromatic opacity (κ_ν) depends on f_{ij}

$$\kappa_\nu(i \rightarrow j) = \frac{\pi e^2}{mc} N_i f_{ij} \phi_\nu \quad (1)$$

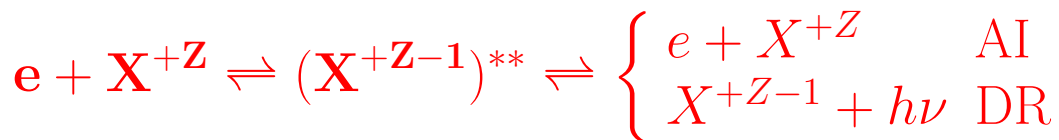
N_i = ion density in state i, ϕ_ν = profile factor

- κ includes $\sim 100M$ transitions of mid-Z elements

2. Photoionization - Photon absorption for a bound-free transition: Direct -



3. Autoionization (AI) in photoionization process :



Doubly excited "autoionizing state" \rightarrow resonance

- Photoionization Cross Sections (σ_{PI})

κ_ν depends on σ_{PI}

$$\kappa_\nu = N_i \sigma_{PI}(\nu) \quad (2)$$

κ_ν depends also on processes

- Inverse Bremstrahlung free-free Scattering:

$$h\nu + [X_1^+ + e(\epsilon)] \rightarrow X_2^+ + e(\epsilon'), \quad (3)$$

Cross section - from the elastic scattering matrix elements for electron impact excitation. An approximate expression for the free-free opacity is

$$\kappa_\nu^{ff}(1, 2) = 3.7 \times 10^8 N_e N_i g_{ff} \frac{Z^2}{T^{1/2} \nu^3} \quad (4)$$

where g_{ff} is a Gaunt factor

- Photon-Electron scattering:

a) Thomson scattering when the electron is free

$$\kappa(s\gamma) = N_e \sigma_{Th} = N_e \frac{8\pi e^4}{3m_e^2 c^4} = 6.65 \times 10^{-25} \text{ cm}^2/\text{g} \quad (5)$$

b) Rayleigh scattering when the electron is bound

$$\kappa_\nu^R = n_i \sigma_\nu^R \approx n_i f_t \sigma^{Th} \left(\frac{\nu}{\nu_I} \right)^4 \quad (6)$$

$h\nu_I$ = binding energy, f_t = total oscillator strength associated with the bound electron.

The equation of state (EOS)

- Ionization fractions and level populations of each ion of an element in levels with non-negligible occupation probability.

Rosseland mean $\kappa_R(T, \rho)$:

Harmonic mean opacity averaged over the Planck function, ρ is the mass density (g/cc),

$$\frac{1}{\kappa_R} = \frac{\int_0^\infty \frac{1}{\kappa_\nu} g(u) du}{\int_0^\infty g(u) du},$$

where $g(u)$ is the Planck weighting function

$$g(u) = \frac{15}{4\pi^4} \frac{u^4 e^{-u}}{(1 - e^{-u})^2}, \quad u = \frac{h\nu}{kT}$$

$g(u)$, for an astrophysical state is calculated with different chemical compositions H (X), He (Y) and metals (Z), such that

$$X + Y + Z = 1$$

THEORY: Relativistic Breit-Pauli Approximation

For a multi-electron system,

$$H^{BP}\Psi_E = E\Psi_E \quad (7)$$

the relativistic Breit-Pauli Hamiltonian is:

$$H^{BP} = H^{NR} + H^{\text{mass}} + H^{\text{Dar}} + H^{\text{so}} + \frac{1}{2} \sum_{i \neq j}^N [g_{ij}(so + so') + g_{ij}(ss') + g_{ij}(css') + g_{ij}(d) + g_{ij}(oo')]. \quad (8)$$

where H_{NR} is the nonrelativistic Hamiltonian:

$$H^{NR} = \sum_{i=1}^N \left\{ -\nabla_i^2 - \frac{2Z}{r_i} + \sum_{j>i}^N \frac{2}{r_{ij}} \right\} \quad (9)$$

Relativistic Breit-Pauli R-matrix (BPRM) method

includes the three one-body correction terms:

$$H_{N+1}^{BP} = H_{N+1}^{NR} + H_{N+1}^{\text{mass}} + H_{N+1}^{\text{Dar}} + H_{N+1}^{\text{so}}, \quad (10)$$

$$H^{\text{mass}} = -\frac{\alpha^2}{4} \sum_i p_i^4, \quad H^{\text{Dar}} = \frac{\alpha^2}{4} \sum_i \nabla^2 \left(\frac{Z}{r_i} \right), \quad H^{\text{so}} = \left[\frac{Ze^2 \hbar^2}{2m^2 c^2 r^3} \right] L.S$$

H^{so} splits LS energy in to fine structure levels.

The latest BPRM codes include the two-body Breit interaction term:

$$H^B = \sum_{i>j} [g_{ij}(so + so') + g_{ij}(ss')] \quad (11)$$

Close-coupling Approximation & R-matrix method

- In close coupling (CC) approximation, the ion is treated as a system of ($N+1$) electrons: a target or the ion core of N electrons with the additional interacting ($N+1$)th electron:
- Total wavefunction expansion is expressed as:

$$\Psi_E(e + \text{ion}) = A \sum_i^N \chi_i(\text{ion}) \theta_i + \sum_j c_j \Phi_j(e + \text{ion})$$

$\chi_i \rightarrow$ target ion or core wavefunction

$\theta_i \rightarrow$ interacting electron wavefunction (continuum or bound)

$\Phi_j \rightarrow$ correlation functions of (e+ion)

- The complex resonant structures in the atomic processes are included through channel couplings.
- Substitution of $\Psi_E(e + \text{ion})$ in $H\Psi_E = E\Psi_E$ results in a set of coupled equations
- Coupled equations are solved by R-matrix method
- $E < 0 \rightarrow$ Bound (e+ion) states Ψ_B
- $E \geq 0 \rightarrow$ Continuum states Ψ_F

ATOMIC PROCESSES:
Quantity of Interest - S (Line Strength)

Transition Matrix elements:

$\langle \Psi_B || D || \Psi_{B'} \rangle \rightarrow$ Radiative Excitation
 $\langle \Psi_B || D || \Psi_F \rangle \rightarrow$ Photoionization

$D = \sum_i \mathbf{r}_i \rightarrow$ Dipole Operator

The matrix element reduces to generalized line strength,

$$S = \left| \left\langle \Psi_f \left| \sum_{j=1}^{N+1} r_j \right| \Psi_i \right\rangle \right|^2 \quad (12)$$

PHOTO-EXCITATION AND DE-EXCITATION:
The oscillator strength (f_{ij}) and radiative decay rate (A_{ji}) for the bound-bound transition are

$$f_{ij} = \left[\frac{E_{ji}}{3g_i} \right] S, \quad A_{ji} (\text{sec}^{-1}) = \left[0.8032 \times 10^{10} \frac{E_{ji}^3}{3g_j} \right] S \quad (13)$$

PHOTOIONIZATION:

The photoionization cross section, σ_{PI} ,

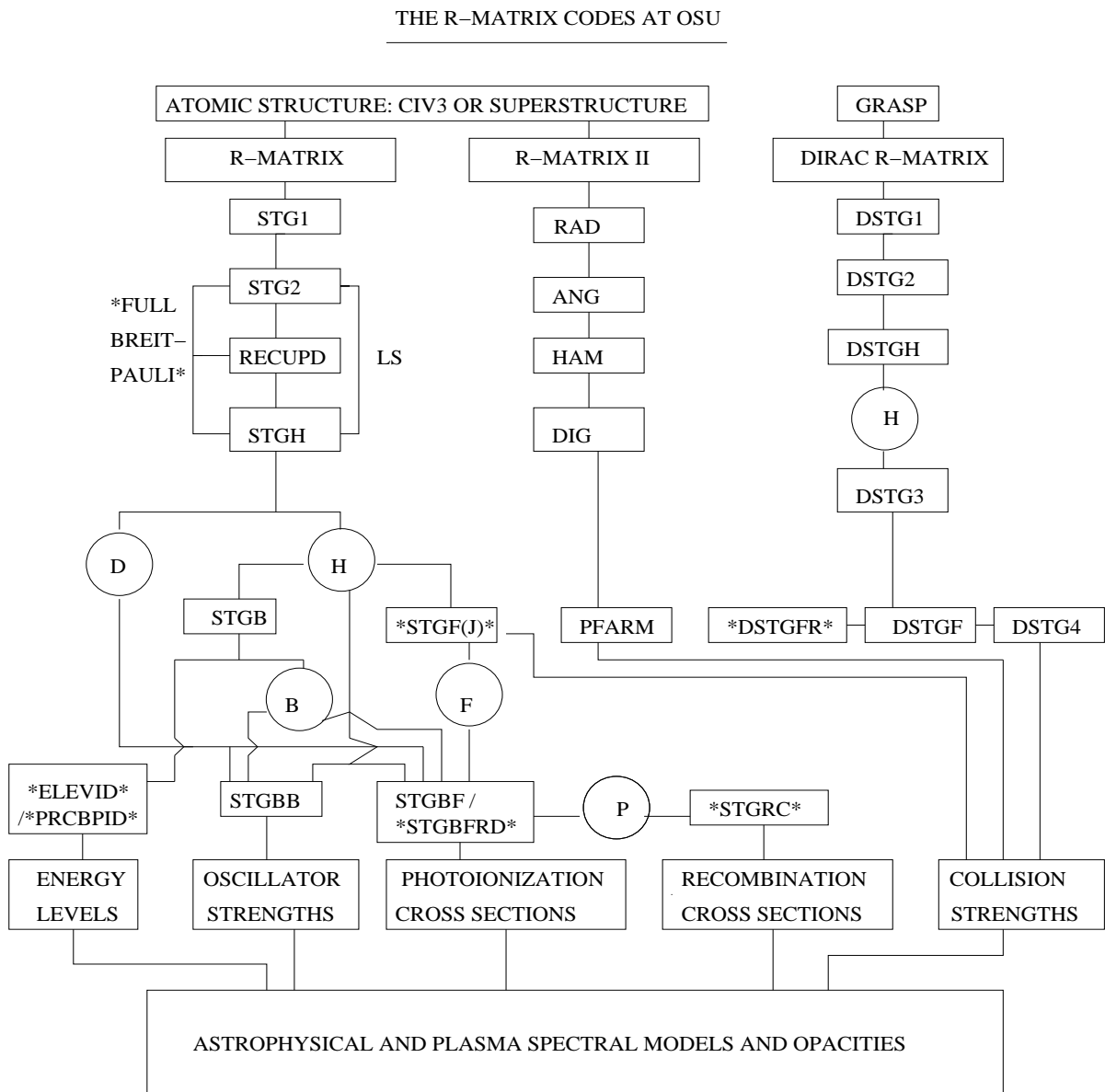
$$\sigma_{PI} = \left[\frac{4\pi}{3c} \frac{1}{g_i} \right] \omega S, \quad (14)$$

$\omega \rightarrow$ incident photon energy in Rydberg unit

R-Matrix Codes For Large-Scale Atomic Calculations at the Ohio Supercomputer Center

VARIOUS COMPUTATIONAL STAGES

- R-matrix calculations can proceed in 3 branches - 1) LS coupling & relativistic Breit-Pauli, 2) LS coupling R-matrix II for Large configuration interaction, 3) DARC for Full Dirac relativistic
- Results - 1) Energy Levels, 2) Oscillator Strengths, 3) Photoionization Cross sections, 4) Recombination Rate Coefficients, 5) Collision Strengths; - Astrophysical Models



RADIATIVE EXCITATIONS & DECAY RATES

(*f*-, *S*, *A*-values for various transitions)

Allowed electric dipole (E1) transitions (BPRM)

- i) Same spin multiplicity dipole allowed ($\Delta j=0,\pm 1$, $\Delta L = 0, \pm 1, \pm 2$, $\Delta S = 0$, parity π changes)
- ii) Intercombination ($\Delta j=0,\pm 1$, $\Delta L = 0, \pm 1, \pm 2$, $\Delta S \neq 0$, π changes)

$$A_{ji}(\text{sec}^{-1}) = 0.8032 \times 10^{10} \frac{E_{ji}^3}{3g_j} S^{E1}, \quad f_{ij} = \frac{E_{ji}}{3g_i} S^{E1}(ij) \quad (15)$$

- Relativistic BPRM calculations include both types in contrast to LS coupling which includes same spin multiplicity dipole allowed only

Forbidden transitions (Atomic Structure)

- i) Electric quadrupole (E2) transitions ($\Delta J = 0, \pm 1, \pm 2$, parity does not change)

$$A_{ji}^{E2} = 2.6733 \times 10^3 \frac{E_{ij}^5}{g_j} S^{E2}(i,j) \text{ s}^{-1}, \quad (16)$$

- ii) Magnetic dipole (M1) transitions ($\Delta J = 0, \pm 1$, parity does not change)

$$A_{ji}^{M1} = 3.5644 \times 10^4 \frac{E_{ij}^3}{g_j} S^{M1}(i,j) \text{ s}^{-1}, \quad (17)$$

iii) Electric octupole (E3) transitions ($\Delta J = \pm 2, \pm 3$, parity changes)

$$A_{ji}^{E3} = 1.2050 \times 10^{-3} \frac{E_{ij}^7}{g_j} S^{E3}(i, j) \text{ s}^{-1}, \quad (18)$$

iv) Magnetic quadrupole (M2) transitions ($\Delta J = \pm 2$, parity changes)

$$A_{ji}^{M2} = 2.3727 \times 10^{-2} \text{ s}^{-1} \frac{E_{ij}^5}{g_j} S^{M2}(i, j). \quad (19)$$

- Under the Iron Project, the above transitions are being calculated in the relativistic Breit-Pauli approximation

LIFETIME:

The lifetime of a level can be obtained from the A-values,

$$\tau_k(s) = \frac{1}{\sum_i A_{ki}(s^{-1})}. \quad (20)$$

”All new calculations are resulting in larger number of accurate transitions for more accurate opacities”

Fe XIX: Comparison of forbidden transitions

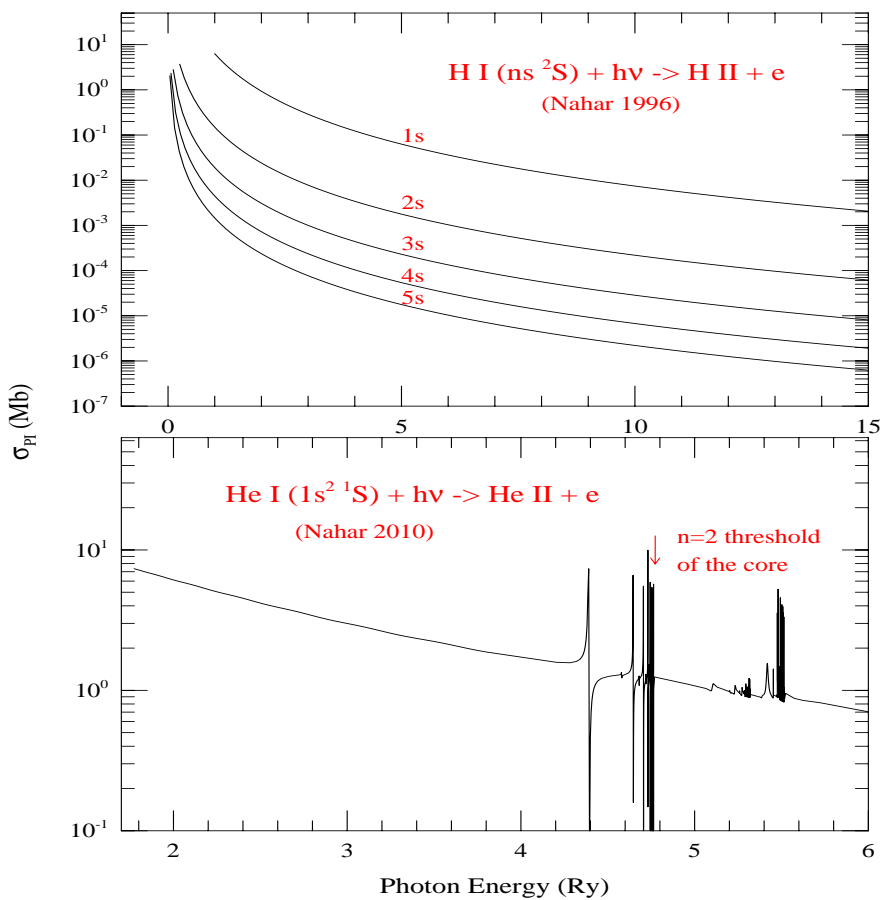
- Good agreement with existing results

E2, E3, M1, M2 transitions: a- Cheng et al (1979),
b- Loulergue et al (1985), c- Jonauskas et al (2004).

λ (\AA)	$A(\text{s}^{-1})$ (Others)	$A(\text{s}^{-1})$ (present)	$C_i - C_j$	$SL\pi$ i-j	g i-j
424.26	1.50e+05 ^a :C,1.39e+05 ^c	1.41e+5	$2s^22p^4 - 2s^22p^4 : M1$	${}^3P - {}^1S$	3- 1
592.234	6.00 ^a :E,6.18 ^c	6.0	$2s^22p^4 - 2s^22p^4 : E2$	${}^3P - {}^1D$	5- 5
592.234	1.73e+04 ^a :C,1.69e+04 ^c	1.67e+4	$2s^22p^4 - 2s^22p^4 : M1$	${}^3P - {}^1D$	5-5
639.84	4.9e+01 ^a :E,4.83e+01 ^c	4.92e+1	$2s^22p^4 - 2s^22p^4 : E2$	${}^1D - {}^1S$	5-1
1118.06	0.611 ^a :E,0.614 ^c	0.635	$2s^22p^4 - 2s^22p^4 : E2$	${}^3P - {}^3P$	5-3
1118.06	1.45e+04 ^a :C,1.42e+04 ^c	1.46e+4	$2s^22p^4 - 2s^22p^4 : M1$	${}^3P - {}^3P$	5-3
1259.27	6.70e+02 ^a :D,6.99e+02 ^c	6.51e+2	$2s^22p^4 - 2s^22p^4 : M1$	${}^3P - {}^1D$	3- 5
1328.90	0.491 ^a :E,0.509 ^c	0.502	$2s^22p^4 - 2s^22p^4 : E2$	${}^3P - {}^3P$	5- 1
2207.8	4.820e+03 ^b :C	4.96e+03	$2s2p^5 - 2s2p^5 : M1$	${}^3P^o - {}^3P^o$	3- 1
7045	4.0e+01 ^a : C	41.0	$2s^22p^4 - 2s^22p^4 : M1$	${}^3P - {}^3P$	1- 3
353.532	9.4e+03 ^b : D	8.79e+03	$2s2p^5 - 2s2p^5 : M1$	${}^3P^o - {}^1P^o$	3-3
420.911	7.7e+03 ^b :D,8.06e+03 ^c	7.31e+03	$2s2p^5 - 2s2p^5 : M1$	${}^3P^o - {}^1P^o$	1-3

PHOTOIONIZATION

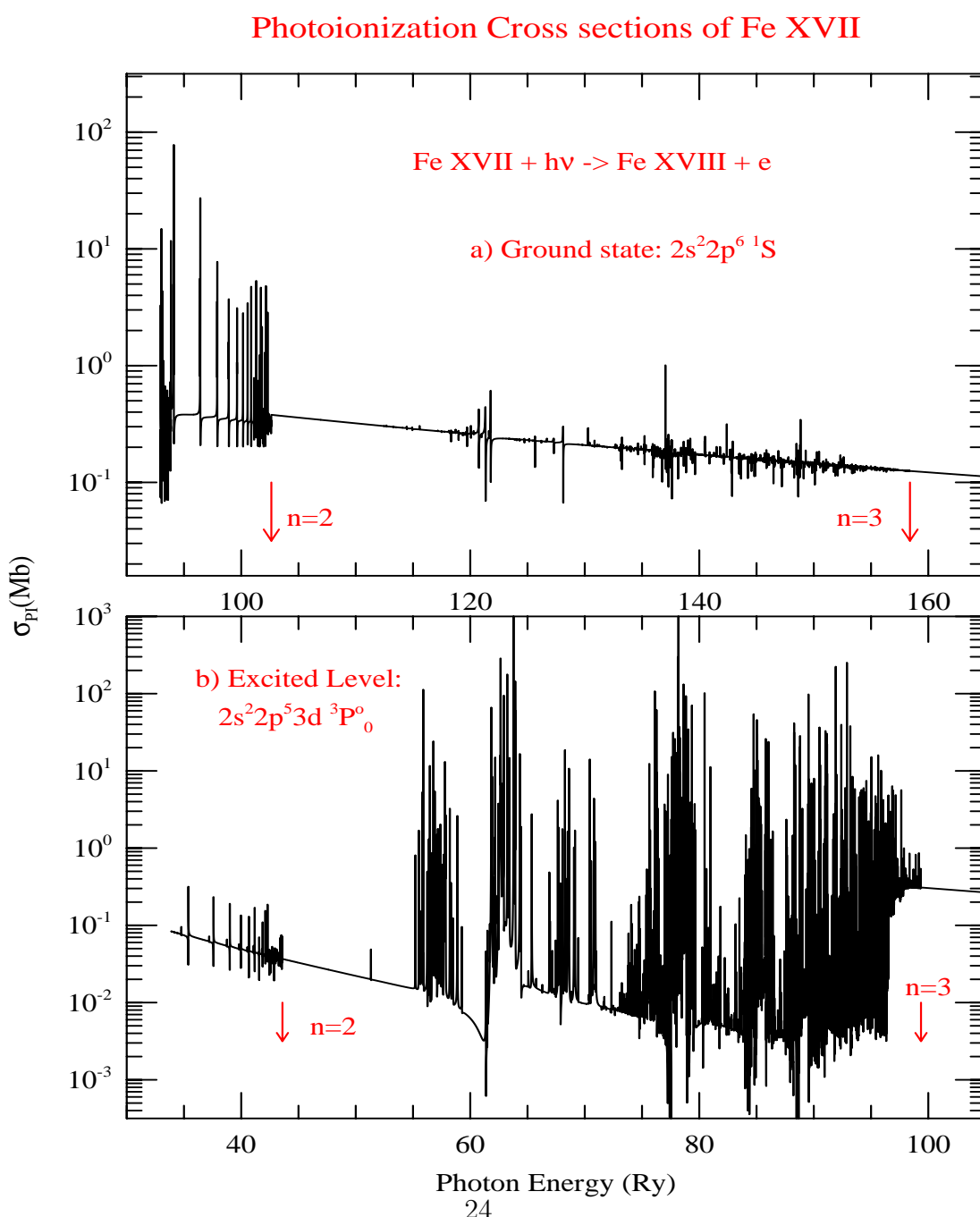
- Atomic system with more than 1 electron - resonances in photoionization
- Earlier calculations for σ_{PI} under the OP considered low-lying resonances
- Core excitations to higher states - assumed weaker and hydrogenic
- Fine structure introduce new features
- New calculations under the IP \rightarrow new and dominating features not studied before - these should change the current calculated opacities and resolve the gap



PHOTOIONIZATION CROSS SECTION: Fe XVII

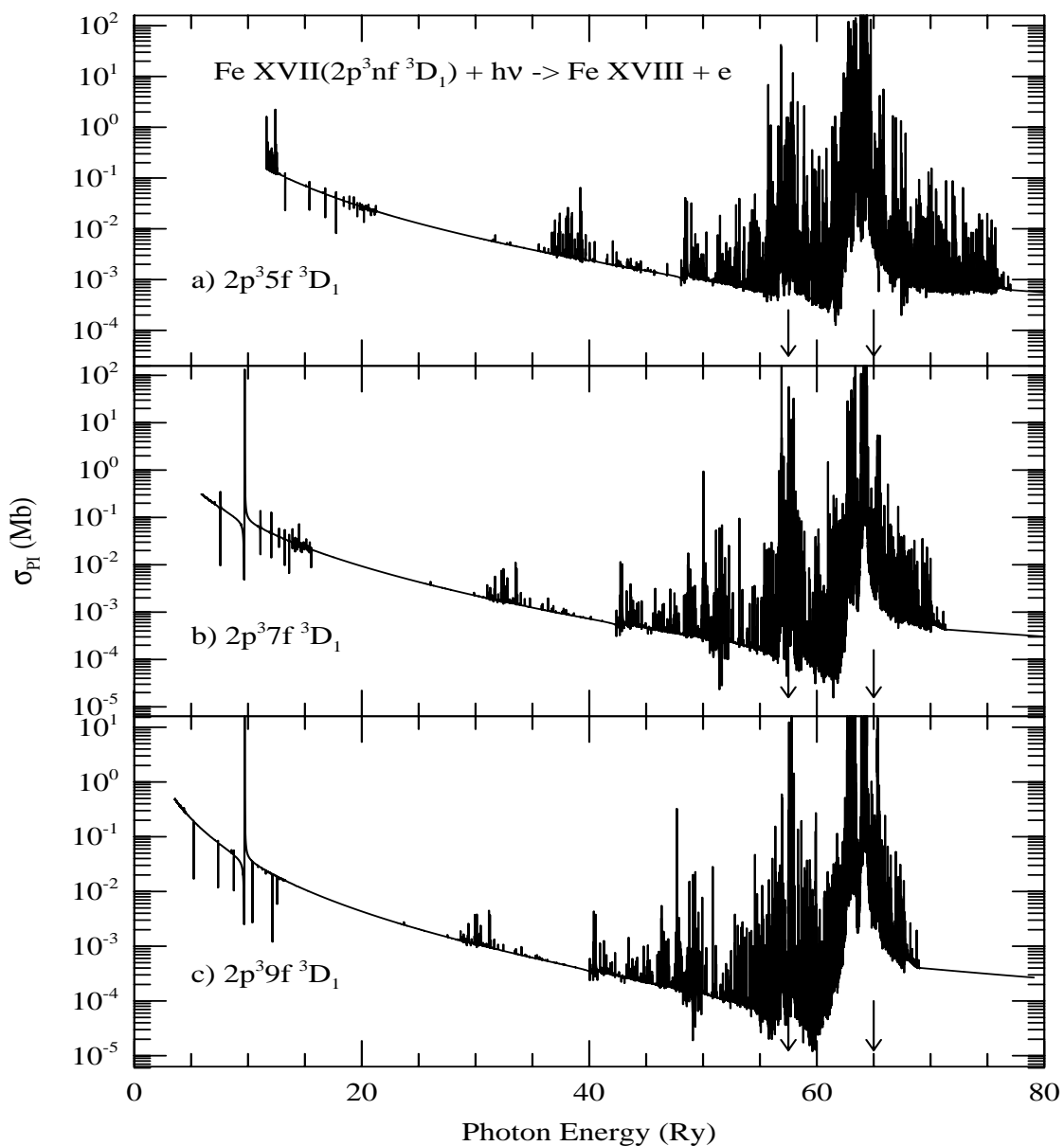
- Top: Ground level: $n=2$ resonances are important
- Bottom: Excited levels: $n=3$ resonances are important

Arrows point energy limits of $n=2$ & 3 core states



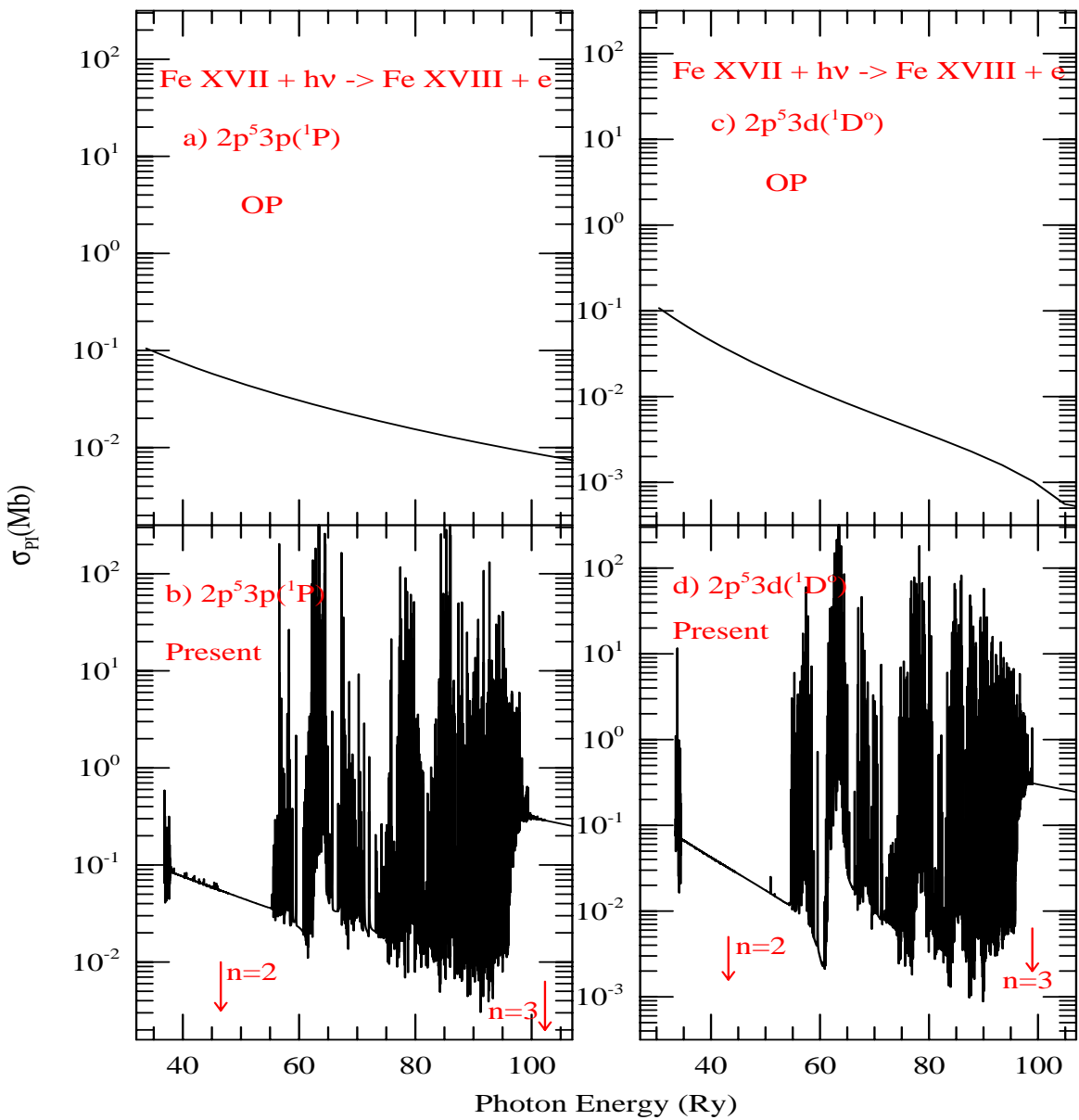
Fe XVII: PEC (Seaton) RESONANCES IN σ_{PI} :

- PEC (Photo-Excitation-of-Core) resonances appear for single valence-electron excited levels
- Appear at energies for core dipole transitions
- PEC resonances are strong and enhance the background cross sections by orders of magnitude
- PEC resonances will affect photoionization and recombination rates of high temperature plasmas



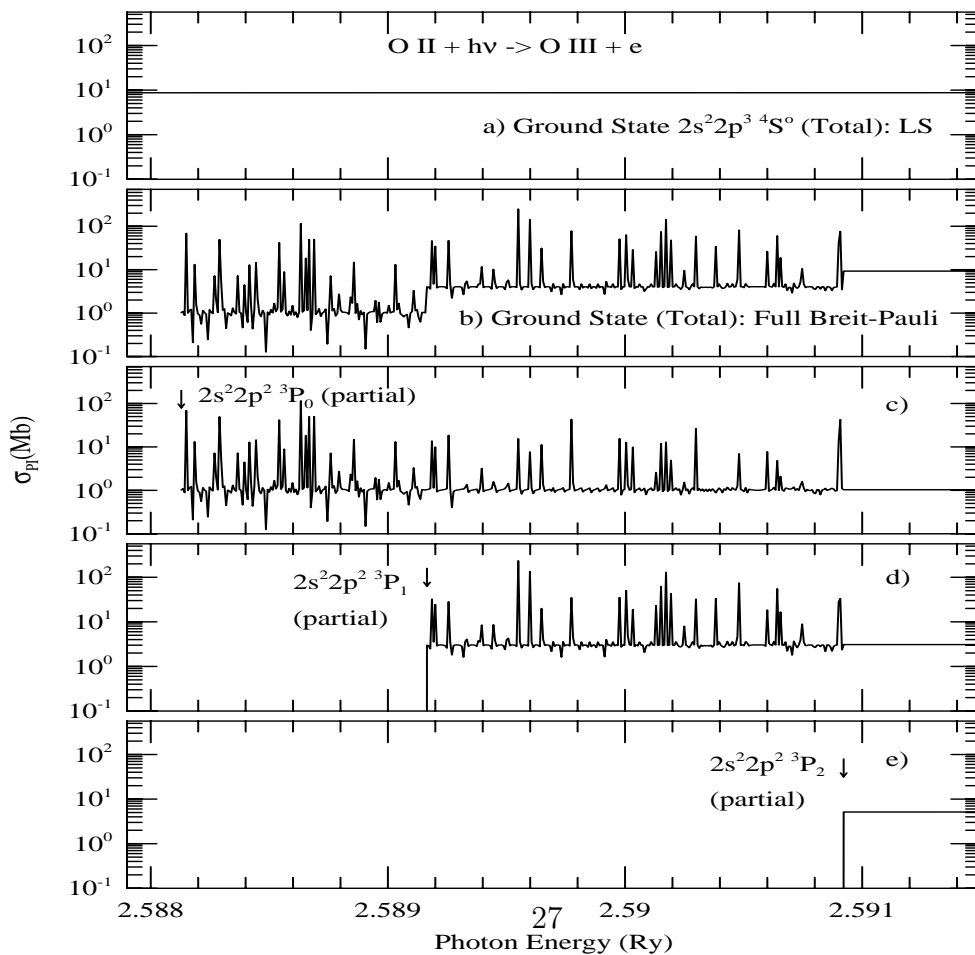
COMPARISON OF σ_{PI} : Fe XVII

- (a,b) level $2p^53p(^1P)$ & (c,d) level $2p^53d(^1D^o)$
- Present σ_{PI} (Nahar et al 2010) show importance of resonant effects compared to those from the Opacity Project (OP)
- Without $n=3$ core states, σ_{PI} is considerably underestimated



Relativistic Fine Structure Effects on Low Energy Photoionization

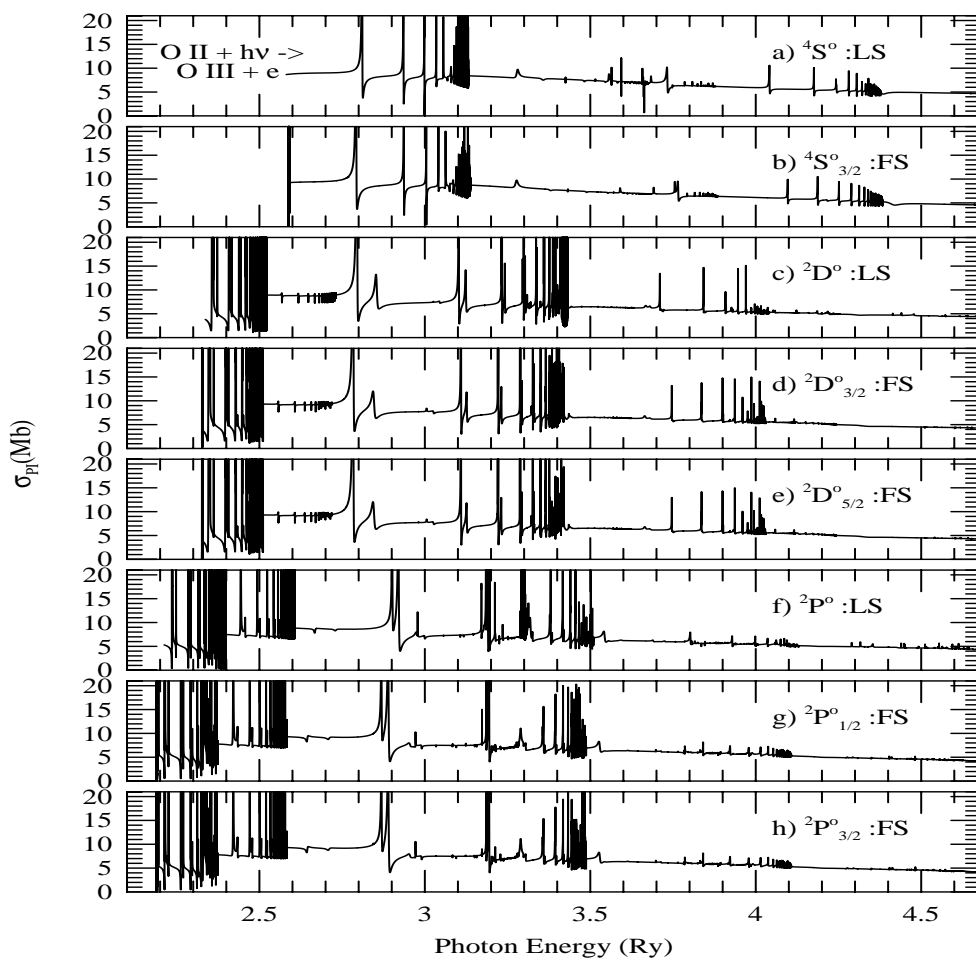
- More important in low energy region
- Introduce features not allowed in LS coupling; Ex. O II (Nahar et al. 2010)
- Figure: σ_{PI} of ground state $2s^22p^3(^4S_{3/2}^o)$
- a) σ_{PI} (LS)- a smooth line (Nahar 1998)
- b) total σ_{PI} in full Breit-Pauli - background jump at each core ionization threshold 3P_0 , 3P_1 , & 3P_2 (latest BPRM)
- Resonances at $^3P_{0,1}$ ionization - due to couplings of fine structure channels



Fine Structure Effects on Low Z ion: O II

Nahar et al. 2010

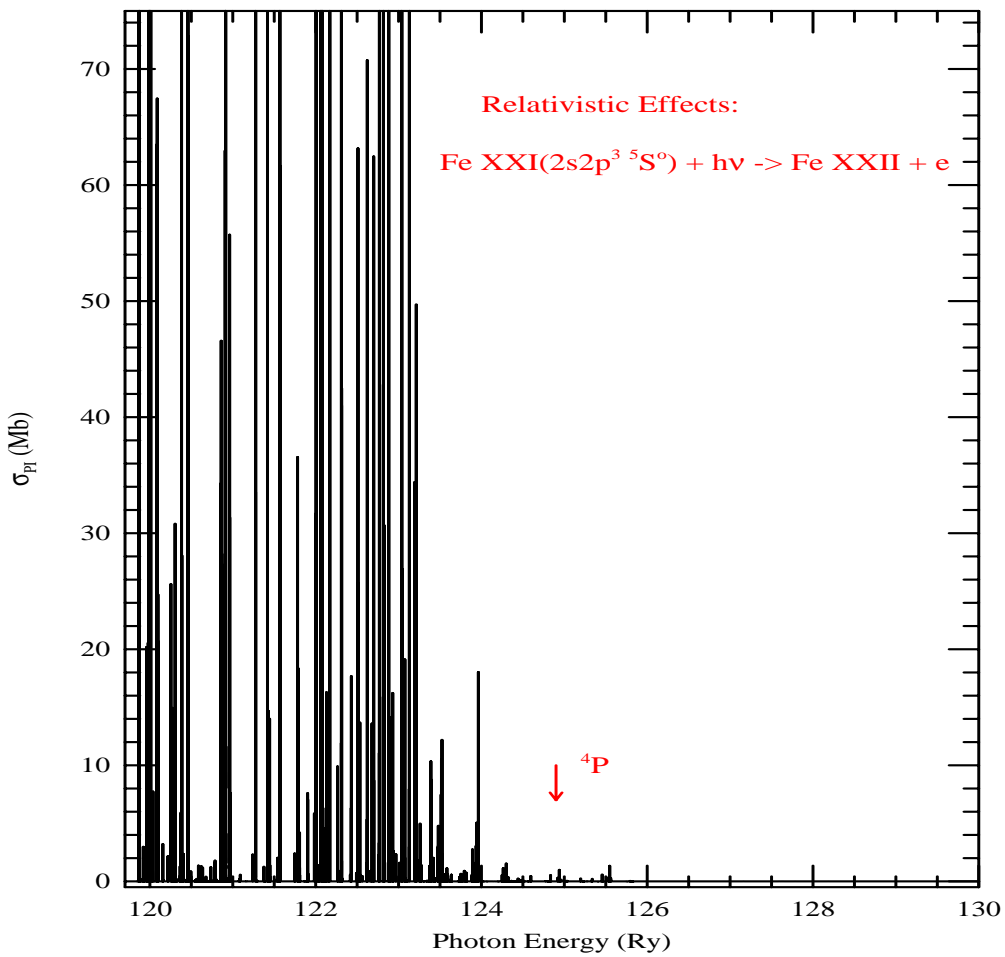
- $\sigma_{PI}(LS)$ of O II states: LS coupling similar to fine structure except at thresholds
- $\sigma_{PI}(LS)$ showed good agreement with experiment (ALS: Covington et al. 2001)
- However, problem with O II abundance at low T astrophysical plasmas remains
- Low energy structure in $\sigma_{PI}(FS)$ is expected to narrow the difference gap



Observed Fine Structure Resonances in σ_{PI} of Fe XXI

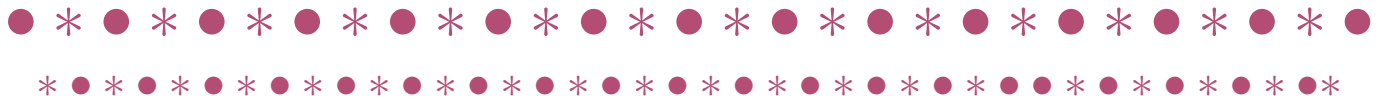
- σ_{PI} of excited $2s2p^3(5S_2^0)$ state (Nahar 2008)
- Strong resonant structures below the arrow - from relativistic fine structure couplings, not allowed in LS coupling
- Observed in recombination spectrum
- These will increase the elemental opacities, and decrease the abundances agreeing with the new findings

Total Photoionization Cross Sections of Fe XXI



CONCLUSION

1. There is a lack of large amount of highly accurate atomic data
2. Solar elemental abundances are widely discordant
3. Z-pinch experiments reveal problems in existing models
4. High precision opacity is crucial to understand astrophysical conditions
5. Consideration of accurate radiative transitions and photoionization resonances due to highly excited core states are essential for more accurate opacity



New TEXTBOOK - Bridging Physics & Astronomy:

”ATOMIC ASTROPHYSICS AND SPECTROSCOPY”

Anil K. Pradhan, Sultana N. Nahar
(Cambridge University Press, 2010)



Contents

- 1 Introduction**
- 2 Atomic Structure**
- 3 Atomic Processes**
- 4 Radiative Transitions**
- 5 Electron-Ion Collisions**
- 6 Photoionization**
- 7 Electron-Ion Recombination**
- 8 Multi-Wavelength Emission Spectra**
- 9 Absorption Lines and Radiative Transfer**
- 10 Stellar Properties and Spectra**
- 11 Opacity and Radiative Forces**
- 12 Gaseous Nebulae and H II Regions**
- 13 Active Galactic Nuclei & Quasars**
- 14 Cosmology**

Physics

Astronomy

